



www.sciencemag.org/cgi/content/full/science.1242902/DC1

Supplementary Material for

Low Upper Limit to Methane Abundance on Mars

Christopher R. Webster,* Paul R. Mahaffy, Sushil K. Atreya, Gregory J. Flesch,
Kenneth A. Farley, the MSL Science Team

*To whom correspondence should be addressed. E-mail: chris.r.webster@jpl.nasa.gov

Published 19 September 2013 on *Science* Express
DOI: 10.1126/science.1242902

This PDF file includes:

Materials and Methods

Figs. S1 to S5

Tables S1 to S3

References (26, 27)

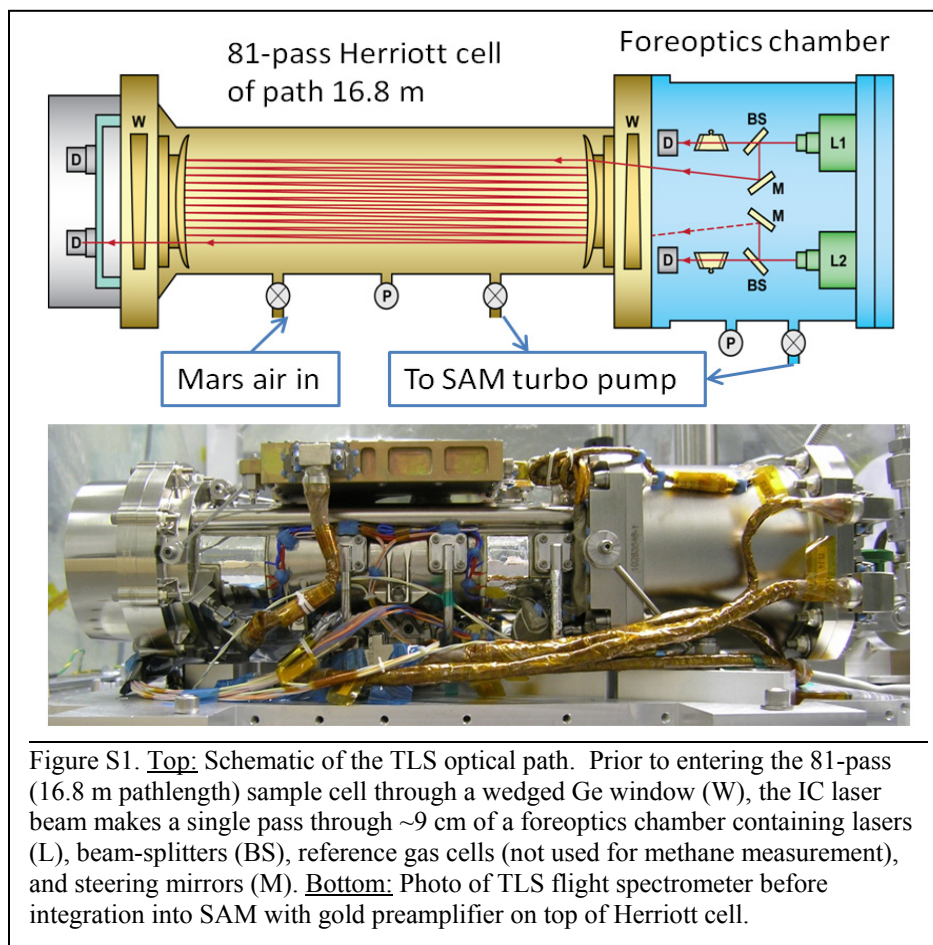
SUPPLEMENTAL INFORMATION:

Low Upper Limit to Methane Abundance on Mars

C. R. Webster, P. R. Mahaffy, S. K. Atreya, G. J. Flesch and K. A. Farley

The Tunable Laser Spectrometer (TLS) in the Sample Analysis at Mars (SAM) instrument suite on the Curiosity Rover

This instrument has been previously described in detail (12, 13). Fig. S1 below emphasizes the optical layout for the methane measurement.



Methane spectroscopy and laser parameters:

The TLS interband cascade (IC) laser scans through a unique fingerprint of seven spectral lines in the ν_3 band: three $^{12}\text{CH}_4$ lines associated with R(3) and four subsequent $^{13}\text{CH}_4$ lines associated with R(3) transitions. Table S1 below lists the three $^{12}\text{CH}_4$ lines used for this study, as identified by both the HITRAN data base (26) and laboratory measurements. We create the labels e, f, g for these three lines, where the g line is strongest, and both e and f are about half the intensity of the g line.

Spectral line center (cm ⁻¹)	Line-strength at 296 K (cm ⁻¹ /molecule·cm ⁻²)	Ground-state energy (cm ⁻¹)	Assignment	Label
3057.687285	2.085E-19	62.8781	R(3)	g
3057.726529	1.245E-19	62.8768	R(3)	f
3057.760524	1.245E-19	62.8757	R(3)	e

The IC laser was developed at JPL, and operated near 245 K stabilized by a two-stage TEC cooler producing single-mode (>99%) continuous-wave output power with a linewidth retrieved from low-pressure (Doppler limited) spectra of ~10 MHz. This light was collimated using an efficient triple-lens collimator to produce ~1 mW laser power that passes through the foreoptics chamber then into the sample (Herriott) cell. Prior to entering the Herriott cell, the beam was attenuated by a factor of ~20 by a thin mylar sheet (not shown in Fig. S1) to reduce optical fringing and detector non-linearity. We note that the pre-launch settings for the TEC and laser current scans (used for calibration also) have not been changed and the target spectral line positions remain in our scan window. Very small (~linewidth) variations in the spectral line position are seen depending on the Curiosity heat ramp behavior, but we observe and track the methane lines continually for each spectrum through the simultaneously-recorded reference cell detector; the tracked methane spectrum arises from residual methane gas in the foreoptics chamber.

Evolved Gas Analysis Spectrum of Figure 1:

In Figure 1 we presented actual flight spectra downloaded from Curiosity rather than showing calculated HITRAN spectra. Spectra C and D are from the methane analysis presented here, but spectra A and B are from a different unrelated experiment on Mars in which a rock sample is heated (Evolved Gas Analysis (EGA) run) in a pyrolysis oven to produce evolved gas fed to TLS that was observed to contain methane. These spectra are shown here in part because they were taken AFTER the atmospheric methane runs and show that our CH₄ lines have not moved, and the instrument continues to work well with consistent capability to detect methane. The EGA spectra of Fig 1 (A, B) show the location of ¹²CH₄ and ¹³CH₄ lines in both the direct absorption and second harmonic (2f) spectrum.

Description of the Difference Method:

We determine Mars methane abundances by differencing full cell and empty cell results (not spectra), as described below. In a typical run on one sol, we collect (downlink) 26 empty cell spectra (2 minutes on board averaged each) followed by 26 full cell, then a few more empty for return-to-zero check. Cell temperatures and pressures are extremely stable during the complete sol run and contribute negligibly to our results (see later). We chose to record relatively long periods of continuous empty or full spectra to make sure that no drift (growth or loss) in retrieved methane abundance was observed during the run. We record sequential 2-minute empty cell spectra for ~1 hour followed by ~1 hour of sequential full cell spectra. We do not difference full-empty spectra before processing. Rather, with powerful computing resources now available, we process each of our 3 methane lines separately in each and all of our 2-minute spectra (by comparison with HITRAN calculations described below), then produce a combined efg-line average abundance for each spectrum that becomes a single raw 2-minute data point. Then, after applying common calibration factors and error contributions, we compare statistically the empty and full cell results for all the sols after normalizing to the empty cell mean values.

Direct and Second-harmonic (2f) Spectra

TLS is designed to simultaneously produce both direct absorption and second harmonic (2f) spectra, as is standard for commercial and laboratory tunable laser spectrometers (27). Tunable laser spectrometers “scan” through spectral lines by applying a current ramp (usually saw-tooth) to the laser that through junction heating changes the wavelength by a small amount, the ramp repeated typically every one second (as done in TLS).

In direct absorption, absorption line depths that indicate gas abundance are measured as dips in the large light level on the detector as the laser is scanned. For very weak absorptions of ~1% or less (due to low gas amounts, too small path lengths or gas pressures, etc., and as expected for low methane (<20 ppbv) amounts) it is challenging for electronics and dynamic range to measure small changes in a large signal, and a “harmonic” detection is preferred. In harmonic detection, the very narrow laser linewidth (much narrower than the gas absorption line) is modulated (“dithered”) at high frequency (say 10 kHz) by applying a sinusoidal component to the laser current ramp (increasing laser current is the normal method of tuning the laser across the spectral scan) with an amplitude that is small compared to the gas linewidth. So, if we modulate at 10 kHz and look at only the component of the detector signal at 10 kHz (using phase-sensitive detection), we would record a first-harmonic or first-derivative 1f spectrum as shown in Fig. S2. Outside the spectral line and at the line center, the laser is jiggling left and right where no difference exists, so it records zero in these places, but has its maximum signals (negative and positive) at the side of the line where the slope is maximum.

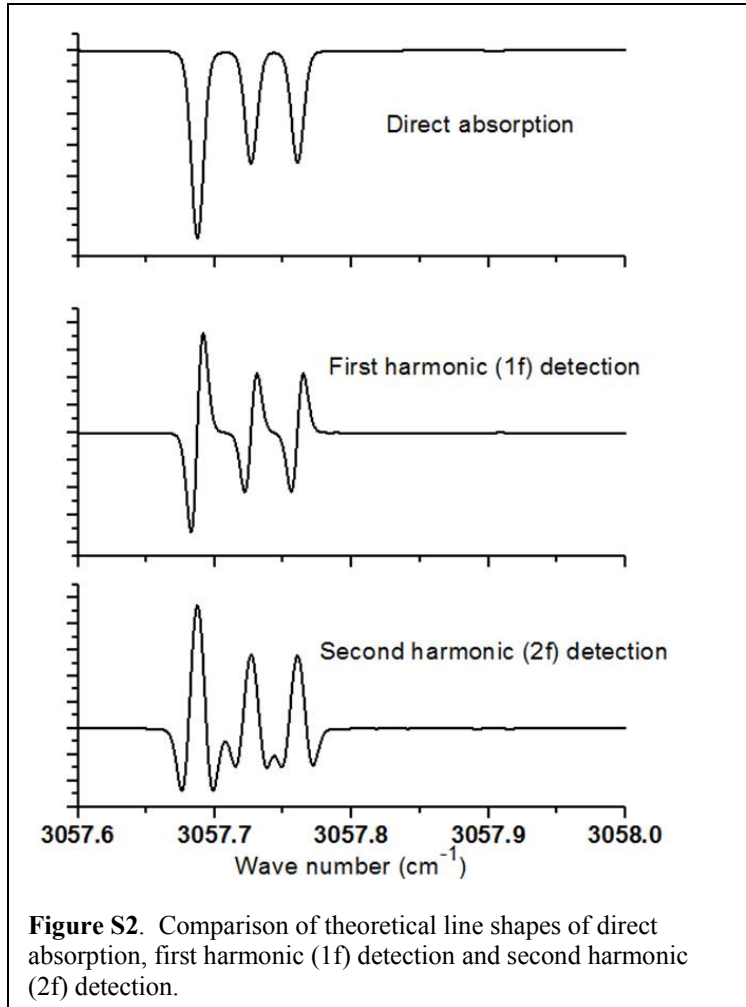


Figure S2. Comparison of theoretical line shapes of direct absorption, first harmonic (1f) detection and second harmonic (2f) detection.

If we now modulate at 10 kHz, but look at the component of the laser light on the detector that is at 20 kHz, we would record (as we do on TLS) the second-harmonic or second-derivative (2f) spectrum seen in Fig. S2. Both 1f and 2f spectral signals are zero-based in amplitude (electronics gain likes that) and move the detection frequency to higher frequency (kHz) compared to the direct (DC) spectrum, where 1/f noise is lower. Thus the harmonic method produces higher signal-to-noise spectra. The 1f spectrum is not usually used since it can have small vertical offsets and the line center position is a zero-crossing rather than a peak. The 2f spectrum is preferred since it has its peak in the same place as the direct absorption spectrum, and moves the detection regime to the higher (20 kHz) frequency.

Spectral Data Processing

The Beer-Lambert law models the optical transmission of light through an absorbing medium:

$$I_{\nu} = I_0 e^{-k(\nu)\rho l}$$

where I_{ν} is the transmitted light intensity at frequency ν , I_0 is the incident light intensity, $k(\nu)$ is a line shaping function that may be Doppler, Lorentzian, or Voigt, although the Doppler lineshape is a close approximation at Mars atmospheric pressures. ρ is the number density and l is the path length in cm. We use this model to determine the abundances of individual absorption lines present in our sampled measurements. The model needs many input spectral parameters for temperature dependence, air broadening, ground state energy, etc., and we use the HITRAN database for this information (26). Direct absorption spectra produce good results for gases that have line center absorption depths of ~1% or greater. For higher sensitivity, we add a modulation to the laser current and then demodulate the returning detector signal at twice that frequency. This effectively gives us a second harmonic or 2f

spectrum in which sensitivities of up to 2 parts in 10^5 are possible. See the section above and also Webster et al. (27) for a complete discussion.

Laser Power Normalization and Wave Number Scale

For a given channel (either CH₄ or CO₂/H₂O), TLS returns 3 spectra from the Herriott cell “science” detector, and 3 spectra from the reference channel detector. For both the Herriott cell and reference channel spectra, these 3 spectra are the direct absorption spectrum, the 2f spectrum, and a high-gain 2f spectrum. Our methane analysis is done using the 2f spectrum that is normalized to laser power from the direct absorption spectrum and mapped to a wave number scale using the reference detector signals. The high-gain 2f spectrum is not used since with only moderate gain increase (x16) it duplicates the 2f spectrum in signal-to-noise ratio but suffers from dynamic range restriction.

TLS also returns reference detector spectra recorded simultaneously with those from the science detector, and these are used to track the methane lines to provide the wave number scale for later processing. The methane signal (spectra) detected by the reference detector (located inside the foreoptics, as shown in Fig. S1) is due to residual methane in the foreoptics. The foreoptics contribution to the science spectrum is equivalent to about 90 ppbv for sols 79-292. The 2-stage thermoelectric cooler on the IC laser keeps the lines in the same position during the scans, with drifts in line positions over all sols of only about 1-2 linewidths that are tracked successfully.

For an amount of gas at a given pressure and temperature, the model will predict the depth and width (distribution in wave number) of the absorption by the gas sample for all sampled frequencies, allowing us to then compare our recorded spectra to the spectra produced by the model. But, in order to make this comparison, we must first normalize the recorded data. This process that takes level 0 data (spectra) and produces level 1 data (spectra) entails:

1. Removing a “null pulse” which is a measurement of the background light taken with the laser off, and recorded during every one second spectrum that is averaged on board for our 2-minute downlinked spectrum. This allows us to determine the direct absorption with respect to a percentage of transmitted light (i.e. 1% absorption: 99% transmission).
2. Removing any DC offsets in the harmonic spectra (described below).
3. Fit the baseline of the spectra. This sloping baseline results from the fact that the laser output power increases as it tunes through different wave numbers.
4. Assign a wave number (cm⁻¹) scale to the real spectra. We do this by using easily identifiable peaks of known wave number.

Once the raw spectra (level 0 data) are normalized (Fig. S3) as level 1 data, we can then use the HITRAN model to scale our real world data.

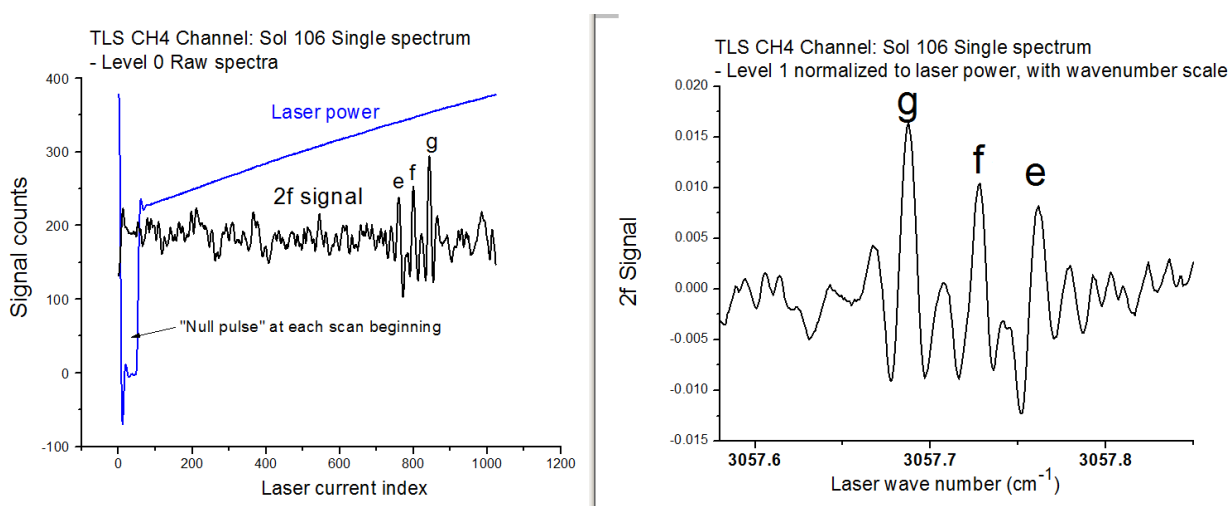


Fig. S3. Example of normalization of a real single spectrum (2 min.) downloaded for sol 106. The methane triplet lines e, f, g can be identified from Table S1 above. The left panel is the complete level 0 spectra, whereas the right panel that shows level 1 data (same 2-min. spectrum normalized to power and given wave number scale) has been

expanded in wave number to show the methane lines used and the occurrence of optical interference fringes that limit the detection method for a single 2-min. spectrum.

Producing Abundances

Using temperatures and pressures from our instrument for input, we iteratively run the model, varying the abundance in a converging algorithm until the synthetic spectra for the single line is the same size as our real spectrum (within some determined threshold). The convergence criteria are set to optimize for the 2f spectra.

For the methane analysis, we generate two results, one named “peak-to-peak” that returns the peak-to-peak signal amplitude (actually central peak to lobe-average) values, and a second named “integral” that returns the area of the 2f line between and above the bottom lobe minima positions (wave number). The peak-to-peak method finds the signal amplitude of the 2f maximum and lobe minima average, and is our preferred method since it produces somewhat lower scatter in our data, although results for either method are very close. The integral method, which is used for retrieving H, C, O isotope ratios (19) uses the following algorithm:

1. Find the global max of the 2f absorption spectra (peak)
2. Find the two local minima (2f lobes)
3. Fit a line between the two lobes
4. Using the lobes as integration boundaries, find the area between the fitted line and the spectra for both the direct and 2f spectra. Ratio this area between real and synthetic spectra and if ratio is outside the convergence threshold, iterate with new abundance.

Once the measurements converge, we ratio the resulting areas of the real spectra to the synthetic spectra which has a known abundance. For both methods, using the same laser modulation and gain throughout (pre-launch calibration and all Mars measurements), we relate the 2f signal size to the direct absorption size through calibration as described below, and like any flight project, we rigorously run our experiment as tested and calibrated pre-launch.

Calibration:

When analyzing direct absorption spectra with known pressure, temperature and pathlength, a Beer’s law calculation using spectral line parameters from HITRAN can in theory provide the gas abundance without the need for calibration gases (i.e. someone else did the work when they created the data base). However, calibration gases serve the dual purpose of verifying the spectrometer response (a check of pathlength or number of passes in a cell, laser linewidth, pressure, mode purity, temperature, saturation, etc.) and also giving a direct calibration (relationship) between the direct absorption and the 2f channel with its various different gain stages.

The relative methane abundances reported here are calibrated using NIST-traceable methane in air provided by the NOAA-CMDL laboratory (provided by Jim Elkins group) specified to contain 88 ± 0.5 ppbv. By injecting this gas into the TLS Herriott cell during pre-launch calibration runs of TLS and SAM in the NASA GSFC environmental chamber, we record both direct absorption and 2f signal sizes using the same conditions (e.g. laser scan, modulation, flight electronics and software, Herriott cell temperature and pressure, ramp heater) used on Mars. During the calibration run, the foreoptics is pumped out so that there is no contribution from foreoptics gas. The path length of the Herriott cell was verified to be 81 passes based on direct absorption measurements of these same methane lines using a second calibration cylinder (same provider) at 1800 ppbv. In addition, by adding pure methane gas at low pressures so that the lines are bleached to zero light transmission at line centers, the mode purity during the scan is verified. No change in alignment or detector signal sizes has been detected since pre-launch. Normalizing the mean value retrieved to 88 ppbv gives us a calibration result and uncertainty of 88.0 ± 1.13 ppbv. We note that this absolute uncertainty of ± 1.13 ppbv does not carry forward in our difference method described below, since it would only serve to change the mean value and upper limit slightly (by ~ 1 part in 88).

The foreoptics contribution to the difference method:

The difference method is described in the body of the main paper, and the sequence shown in Fig. S4 below. During the empty or full cell periods, the foreoptics and Herriott cell pressures are very stable; during a typical run (Sol 106) the temperatures and foreoptics pressure are stable to 0.02%, and the Herriott cell pressure during the full cell section is stable to 0.1%.

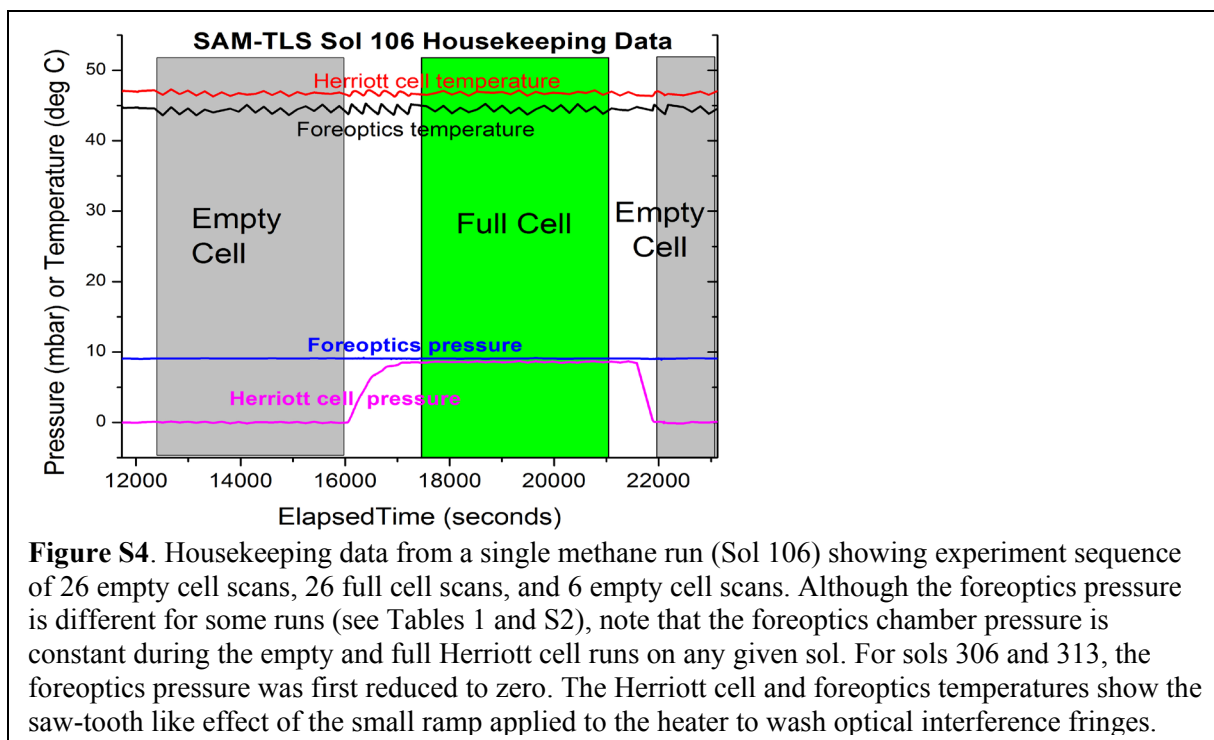


Table S2. Ingest and foreoptics pressures.

Martian Sol after landing	Earth date	Ls (deg)	Gas ingest time and cell pressure (mbar)	Foreoptics pressure (mbar)
79	Oct 25 th 2012	195.0	Night/8.0	11.5
81	Oct 27 th 2012	196.2	Night/8.0	11.5
106	Nov 27 th 2012	214.9	Night/8.5	10.9
292	June 1 st 2013	328.6	Night/8.7	9.2
306	June 16 th 2013	336.5	Day/8.1	~0
313	June 23 rd 2013	340.5	Night/8.7	~0

During the long pre-launch and cruise phase to Mars, the foreoptics chamber leaked up to a significant pressure (~76 mbar) by the time we arrived at Mars. This pressure included terrestrial “Florida air” from the launch site that contained significant terrestrial methane gas (~10 ppmv) that showed up as a large methane signal (spectrum) on the Herriott cell science detector for both “empty” and “full” Herriott cell data, since the beam made one pass through the 9-cm length of the foreoptics. Moreover, our first attempts to measure methane on Mars showed methane spectra that increased in size with time during the empty and full cell scans that we attributed to diffusion (leakage) of the foreoptics methane gas into the Herriott cell during the run. Results from these runs made before sol 79 were discarded and not included in the analysis. To reduce the foreoptics contribution, we pumped down the foreoptics chamber in a series of steps for subsequent sol runs (80, 33, 11.5 mbar) until at 11.5 mbar we observed no detectable increase (or reduction) in the empty or full cell spectra with time over the run, so that we were confident that the leakage was negligible during the runs to follow. As a matter of good practice, for the last two data sets of sols 306 and 313, we further reduced the foreoptics pressure to close to zero by pumping on the chamber. As the data in Table S3 shows, the results for all 6 sols are consistent within measurement uncertainty. Note that the low foreoptics contribution in sols 306 and 313 reduces the scatter in the data somewhat, as shown in Table S3.

Because of the foreoptics contribution, all of our spectra (empty and full Herriott cell) look somewhat like those in Fig. S3 since (in the absence of significant Martian methane) they are dominated by the foreoptics contribution. We then process them as described above, and then look for differences in the empty and full cell results. Specifically, the “full” cell methane spectra are first processed as if the observed methane spectrum came only from the Herriott

cell, that is, we use the measured Herriott cell pressure and temperature to retrieve a “full cell” methane mixing ratio by comparison with HITRAN. Then for the “empty” cell spectra, we use the same mean temperatures and pressures of the full cell and process the empty cell spectra to reveal the “empty cell” methane mixing ratio. This method makes the difference method most sensitive to Herriott cell methane from Mars, should it be there. If there was no methane on Mars, the empty and full cell results would be identical. If there was 20 ppbv methane on Mars, the full cell result would be 20 ppbv larger than the empty cell result. For sols 79-292, for example, both the empty and full cell results are close to 90 ppbv, and for sols 306 and 313 it is <20 ppbv. For the difference data given in Table 1 and S1, the mean empty cell values for that specific run have been subtracted from the full cell values to provide the resulting Martian methane mixing ratio.

The inlet to the SAM-TLS instrument is a 3/16” internal diameter stainless steel tube heated to 50°C containing a dust filter of sintered Inconel 0.5 micron particles that is located on the rover side ~1 m above the Martian surface, and was pointed at a variety of directions relative to the nominal wind direction.

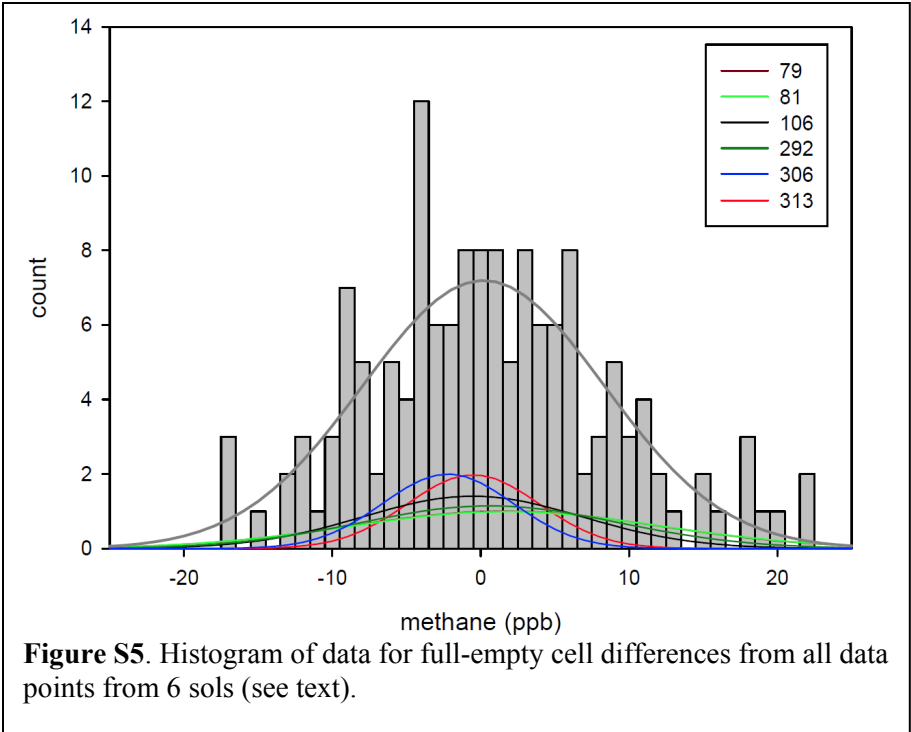
Statistical analysis of data:

The spacecraft returns two-minute averaged signals for each of the three spectral absorption lines given in Table S1. The TLS measurements include methane absorption occurring both in the Herriott cell and along the optical path of the foreoptics prior to entry into the cell, as described in the main text. In our first four sol runs, the foreoptics region had terrestrial air with methane in it, allowing confident identification of the methane absorption lines and continuous monitoring of scan-to-scan line shifts. The foreoptics methane signal also introduces a substantial “blank” signal which must be removed to compute the amount of methane in the Mars atmosphere in the Herriott cell. For the later two sols 306 and 313, the foreoptics were pumped out before hand, and the measured background signals although much lower were treated in exactly the same way for all six sol data comparisons.

We treat each of these lines as a separate estimate of the absorption attributable to methane somewhere along the optic path. These absorptions were converted into an apparent methane mixing ratio in the Herriott cell by assuming that this is the only region in which methane occurs. As shown in Table S3, all of our sol runs except sol 306 were executed to produce 26 full cell points and 32 empty cell points. For sols 292 and 313 the heat ramp monitor showed that we had not quite reached temperature, and the first one and four points, respectively were removed from the analysis. For sol 306, the daytime run and rover power demand meant that the number of full, empty data points was limited to 22 and 18 points. No data points were removed from this analysis. Results for each of the six sol measurements (see Tables 1 and S3) show mean values ranging from -2.2 to 1.7 ppbv. In the absence of any notable difference in the atmospheric methane abundances retrieved on the six sols, we chose to merge the six individual data sets to obtain best estimates of the atmospheric methane amount, its uncertainty, and our upper limit methane value. We thus obtained 147 full cell points and 167 empty cell points that were then statistically analyzed as a single data set. For this calculation we subtracted the mean blank signal on each sol from the measured signals on that sol. The results are shown in Figure S5 as a histogram for the aggregated 6-sol data set. Each individual sol defines a broadly Gaussian distribution and all sols have statistically equivalent variance. These Gaussian distributions are also indicated in Figure S5. The mean empty cell value is by definition zero, while the blank-corrected full cell mean is 0.18 ± 0.67 ppbv. These data imply an upper limit with 95% confidence of 1.3 ppbv for the methane volume mixing ratio of the Martian atmosphere.

Table S3. Statistical data for each sol and 6-sol data treated as single data set.

Martian Sol after landing on Aug 6 th 2012	Number of Full Cell points	Number of Empty Cell points	Mean CH4 value \pm 1SEM (ppbv)
79	26	26	1.62 ± 2.03
81	26	32	1.71 ± 2.06
106	26	31	-0.55 ± 1.45
292	25	31	0.60 ± 1.74
306	22	18	-2.21 ± 0.94
313	22	27	-0.50 ± 0.94
All six sols treated as one data set	147	165	0.18 ± 0.67



Mars Science Laboratory (MSL) Science Team

Aalto University

Osku Kempainen

Applied Physics Laboratory (APL) at Johns Hopkins University

Nathan Bridges, Jeffrey R. Johnson, Michelle Minitti

Applied Research Associates, Inc. (ARA)

David Cremers

Arizona State University (ASU)

James F. Bell III, Lauren Edgar, Jack Farmer, Austin Godber, Meenakshi Wadhwa, Danika Wellington

Ashima Research

Ian McEwan, Claire Newman, Mark Richardson

ATOS Origin

Antoine Charpentier, Laurent Peret

Australian National University (ANU)

Penelope King

Bay Area Environmental Research Institute (BAER)

Jennifer Blank

Big Head Endian LLC

Gerald Weigle

Brock University

Marie Schmidt

Brown University

Shuai Li, Ralph Milliken, Kevin Robertson, Vivian Sun

California Institute of Technology (Caltech)

Michael Baker, Christopher Edwards, Bethany Ehlmann, Kenneth Farley, Jennifer Griffes, John Grotzinger, Hayden Miller, Megan Newcombe, Cedric Pilorget, Melissa Rice, Kirsten Siebach, Katie Stack, Edward Stolper

Canadian Space Agency (CSA)

Claude Brunet, Victoria Hipkin, Richard Léveillé, Geneviève Marchand, Pablo Sobrón Sánchez

Capgemini France

Laurent Favot

Carnegie Institution of Washington

George Cody, Andrew Steele

Carnegie Mellon University

Lorenzo Flückiger, David Lees, Ara Nefian

Catholic University of America

Mildred Martin

Centre National de la Recherche Scientifique (CNRS)

Marc Gailhanou, Frances Westall, Guy Israël

Centre National d'Etudes Spatiales (CNES)

Christophe Agard, Julien Baroukh, Christophe Donny, Alain Gaboriaud, Philippe Guillemot, Vivian Lafaille, Eric Lorigny, Alexis Paillet, René Pérez, Muriel Saccoccio, Charles Yana

Centro de Astrobiología (CAB)

Carlos Armians-Aparicio, Javier Caride Rodríguez, Isaias Carrasco Blázquez, Felipe Gómez Gómez, Javier Gómez-Elvira, Sebastian Hettrich, Alain Lepinette Malvitte, Mercedes Marín Jiménez, Jesús Martínez-Frías, Javier Martín-Soler, F. Javier Martín-Torres, Antonio Molina Jurado, Luis Mora-Sotomayor, Guillermo Muñoz Caro, Sara Navarro López, Verónica Peinado-González, Jorge Pla-García, José Antonio Rodríguez Manfredi, Julio José Romeral-Planelló, Sara Alejandra Sans Fuentes, Eduardo Sebastian Martinez, Josefina Torres Redondo, Roser Urqui-O'Callaghan, María-Paz Zorzano Mier

Chesapeake Energy

Steve Chipera

Commissariat à l'Énergie Atomique et aux Énergies Alternatives (CEA)

Jean-Luc Lacour, Patrick Mauchien, Jean-Baptiste Sirven

Concordia College

Heidi Manning

Cornell University

Alberto Fairén, Alexander Hayes, Jonathan Joseph, Steven Squyres, Robert Sullivan, Peter Thomas

CS Systemes d'Information

Audrey Dupont

Delaware State University

Angela Lundberg, Noureddine Melikechi, Alissa Mezzacappa

Denver Museum of Nature & Science

Julia DeMarines, David Grinspoon

Deutsches Zentrum für Luft- und Raumfahrt (DLR)

Günther Reitz

eINFORMe Inc. (at NASA GSFC)

Benito Prats

Finnish Meteorological Institute

Evgeny Atlaskin, Maria Genzer, Ari-Matti Harri, Harri Haukka, Henrik Kahanpää, Janne Kauhanen, Osku Kempainen, Mark Paton, Jouni Polkko, Walter Schmidt, Tero Siili

GeoResources

Cécile Fabre

Georgia Institute of Technology

James Wray, Mary Beth Wilhelm

Géosciences Environnement Toulouse (GET)

Franck Poitrasson

Global Science & Technology, Inc.

Kiran Patel

Honeybee Robotics

Stephen Gorevan, Stephen Indyk, Gale Paulsen

Imperial College

Sanjeev Gupta

Indiana University Bloomington

David Bish, Juergen Schieber

Institut d'Astrophysique Spatiale (IAS)

Brigitte Gondet, Yves Langevin

Institut de Chimie des Milieux et Matériaux de Poitiers (IC2MP)

Claude Geffroy

Institut de Recherche en Astrophysique et Planétologie (IRAP), Université de Toulouse

David Baratoux, Gilles Berger, Alain Cros, Claude d'Uston, Olivier Forni, Olivier Gasnault, Jérémie Lasue, Qiu-Mei Lee, Sylvestre Maurice, Pierre-Yves Meslin, Etienne Pallier, Yann Parot, Patrick Pinet, Susanne Schröder, Mike Toplis

Institut des Sciences de la Terre (ISTerre)

Éric Lewin

inXitu

Will Brunner

Jackson State University

Ezat Heydari

Jacobs Technology

Cherie Achilles, Dorothy Oehler, Brad Sutter

Laboratoire Atmosphères, Milieux, Observations Spatiales (LATMOS)

Michel Cabane, David Coscia, Guy Israël, Cyril Szopa

Laboratoire de Géologie de Lyon : Terre, Planète, Environnement (LGL-TPE)

Gilles Dromart

Laboratoire de Minéralogie et Cosmochimie du Muséum (LMCM)

François Robert, Violaine Sautter

Laboratoire de Planétologie et Géodynamique de Nantes (LPGN)

Stéphane Le Mouélic, Nicolas Mangold, Marion Nachon

Laboratoire Génie des Procédés et Matériaux (LGPM)

Arnaud Buch

Laboratoire Interuniversitaire des Systèmes Atmosphériques (LISA)

Fabien Stalport, Patrice Coll, Pascaline François, François Raulin, Samuel Teinturier

Lightstorm Entertainment Inc.

James Cameron

Los Alamos National Lab (LANL)

Sam Clegg, Agnès Cousin, Dorothea DeLapp, Robert Dingler, Ryan Steele Jackson, Stephen Johnstone, Nina Lanza, Cynthia Little, Tony Nelson, Roger C. Wiens, Richard B. Williams

Lunar and Planetary Institute (LPI)

Andrea Jones, Laurel Kirkland, Allan Treiman

Malin Space Science Systems (MSSS)

Burt Baker, Bruce Cantor, Michael Caplinger, Scott Davis, Brian Duston, Kenneth Edgett, Donald Fay, Craig Hardgrove, David Harker, Paul Herrera, Elsa Jensen, Megan R. Kennedy, Gillian Krezoski, Daniel Krysak, Leslie Lipkaman, Michael Malin, Elaina McCartney, Sean McNair, Brian Nixon, Liliya Posiolova, Michael Ravine, Andrew Salamon, Lee Saper, Kevin Stoiber, Kimberley Supulver, Jason Van Beek, Tessa Van Beek, Robert Zimdar

Massachusetts Institute of Technology (MIT)

Katherine Louise French, Karl Iagnemma, Kristen Miller, Roger Summons

Max Planck Institute for Solar System Research

Fred Goesmann, Walter Goetz, Stubbe Hviid

Microtel

Micah Johnson, Matthew Lefavor, Eric Lyness

Mount Holyoke College

Elly Breves, M. Darby Dyar, Caleb Fassett

NASA Ames

David F. Blake, Thomas Bristow, David DesMarais, Laurence Edwards, Robert Haberle, Tori Hoehler, Jeff Hollingsworth, Melinda Kahre, Leslie Keely, Christopher McKay, Mary Beth Wilhelm

NASA Goddard Space Flight Center (GSFC)

Lora Bleacher, William Brinckerhoff, David Choi, Pamela Conrad, Jason P. Dworkin, Jennifer Eigenbrode, Melissa Floyd, Caroline Freissinet, James Garvin, Daniel Glavin, Daniel Harpold, Andrea Jones, Paul Mahaffy, David K. Martin, Amy McAdam, Alexander Pavlov, Eric Raaen, Michael D. Smith, Jennifer Stern, Florence Tan, Melissa Trainer

NASA Headquarters

Michael Meyer, Arik Posner, Mary Voytek

NASA Jet Propulsion Laboratory (JPL)

Robert C. Anderson, Andrew Aubrey, Luther W. Beegle, Alberto Behar, Diana Blaney, David Brinza, Fred Calef, Lance Christensen, Joy A. Crisp, Lauren DeFlores, Bethany Ehlmann, Jason Feldman, Sabrina Feldman, Gregory Flesch, Joel Hurowitz, Insoo Jun, Didier Keymeulen, Justin Maki, Michael Mischna, John Michael Morookian, Timothy Parker, Betina Pavri, Marcel Schoppers, Aaron Sengstacken, John J. Simmonds, Nicole Spanovich, Manuel de la Torre Juarez, Ashwin R. Vasavada, Christopher R. Webster, Albert Yen

NASA Johnson Space Center (JSC)

Paul Douglas Archer, Francis Cucinotta, John H. Jones, Douglas Ming, Richard V. Morris, Paul Niles, Elizabeth Rampe

Nolan Engineering

Thomas Nolan

Oregon State University

Martin Fisk

Piezo Energy Technologies

Leon Radziemski

Planetary Science Institute

Bruce Barraclough, Steve Bender, Daniel Berman, Eldar Noe Dobrea, Robert Tokar, David Vaniman, Rebecca M. E. Williams, Aileen Yingst

Princeton University

Kevin Lewis

Rensselaer Polytechnic Institute (RPI)

Laurie Leshin

Retired

Timothy Cleghorn, Wesley Huntress, Gérard Manhès

Salish Kootenai College

Judy Hudgins, Timothy Olson, Noel Stewart

Search for Extraterrestrial Intelligence Institute (SETI I)

Philippe Sarrazin

Smithsonian Institution

John Grant, Edward Vicenzi, Sharon A. Wilson

Southwest Research Institute (SwRI)

Mark Bullock, Bent Ehresmann, Victoria Hamilton, Donald Hassler, Joseph Peterson, Scot Rafkin, Cary Zeitlin

Space Research Institute

Fedor Fedosov, Dmitry Golovin, Natalya Karpushkina, Alexander Kozyrev, Maxim Litvak, Alexey Malakhov, Igor Mitrofanov, Maxim Mokrousov, Sergey Nikiforov, Vasily Prokhorov, Anton Sanin, Vladislav Tretyakov, Alexey Varenikov, Andrey Vostrukhin, Ruslan Kuzmin

Space Science Institute (SSI)

Benton Clark, Michael Wolff

State University of New York (SUNY) Stony Brook

Scott McLennan

Swiss Space Office

Oliver Botta

TechSource

Darrell Drake

Texas A&M

Keri Bean, Mark Lemmon

The Open University

Susanne P. Schwenger

United States Geological Survey (USGS) Flagstaff

Ryan B. Anderson, Kenneth Herkenhoff, Ella Mae Lee, Robert Sucharski

Universidad de Alcalá

Miguel Ángel de Pablo Hernández, Juan José Blanco Ávalos, Miguel Ramos

Universities Space Research Association (USRA)

Myung-Hee Kim, Charles Malespin, Ianik Plante

University College London (UCL)

Jan-Peter Muller

University Nacional Autónoma de México (UNAM)

Rafael Navarro-González

University of Alabama

Ryan Ewing

University of Arizona

William Boynton, Robert Downs, Mike Fitzgibbon, Karl Harshman, Shauna Morrison

University of California Berkeley

William Dietrich, Onno Kortmann, Marisa Palucis

University of California Davis

Dawn Y. Sumner, Amy Williams

University of California San Diego

Günter Lugmair

University of California San Francisco

Michael A. Wilson

University of California Santa Cruz

David Rubin

University of Colorado Boulder

Bruce Jakosky

University of Copenhagen

Tonci Balic-Zunic, Jens Frydenvang, Jaqueline Kløvgaard Jensen, Kjartan Kinch, Asmus Koefoed, Morten Bo Madsen, Susan Louise Svane Stipp

University of Guelph

Nick Boyd, John L. Campbell, Ralf Gellert, Glynis Perrett, Irina Pradler, Scott VanBommel

University of Hawai'i at Manoa

Samantha Jacob, Tobias Owen, Scott Rowland

University of Helsinki

Evgeny Atlaskin, Hannu Savijärvi

University of Kiel

Eckart Boehm, Stephan Böttcher, Sönke Burmeister, Jingnan Guo, Jan Köhler, César Martín García, Reinhold Mueller-Mellin, Robert Wimmer-Schweingruber

University of Leicester

John C. Bridges

University of Maryland

Timothy McConnochie

University of Maryland Baltimore County

Mehdi Benna, Heather Franz

University of Maryland College Park

Hannah Bower, Anna Brunner

University of Massachusetts

Hannah Blau, Thomas Boucher, Marco Carmosino

University of Michigan Ann Arbor

Sushil Atreya, Harvey Elliott, Douglas Halleaux, Nilton Rennó, Michael Wong

University of Minnesota

Robert Pepin

University of New Brunswick

Beverley Elliott, John Spray, Lucy Thompson

University of New Mexico

Suzanne Gordon, Horton Newsom, Ann Ollila, Joshua Williams

University of Queensland

Paulo Vasconcelos

University of Saskatchewan

Jennifer Bentz

University of Southern California (USC)

Kenneth Neelson, Radu Popa

University of Tennessee Knoxville

Linda C. Kah, Jeffrey Moersch, Christopher Tate

University of Texas at Austin

Mackenzie Day, Gary Kocurek

University of Washington Seattle

Bernard Hallet, Ronald Sletten

University of Western Ontario

Raymond Francis, Emily McCullough

University of Winnipeg

Ed Cloutis

Utrecht University

Inge Loes ten Kate

Vernadsky Institute

Ruslan Kuzmin

Washington University in St. Louis (WUSTL)

Raymond Arvidson, Abigail Fraeman, Daniel Scholes, Susan Slavney, Thomas Stein, Jennifer Ward

Western University

Jeffrey Berger

York University

John E. Moores

References and Notes

1. S. K. Atreya, P. R. Mahaffy, H. B. Niemann, M. H. Wong, T. C. Owen, Composition and origin of the atmosphere of Jupiter—an update, and implications for the extrasolar giant planets. *Planet. Space Sci.* **51**, 105–112 (2003). [doi:10.1016/S0032-0633\(02\)00144-7](https://doi.org/10.1016/S0032-0633(02)00144-7)
2. H. A. Michelsen, G. L. Manney, C. R. Webster, R. D. May, M. R. Gunson, D. Baumgardner, K. K. Kelly, M. Loewenstein, J. R. Podolske, M. H. Proffitt, S. C. Wofsy, G. K. Yue, Intercomparison of ATMOS, SAGE II, and ER-2 observations in the Arctic vortex and extra-vortex air masses during spring 1993. *Geophys. Res. Lett.* **26**, 291–294 (1999). [doi:10.1029/1998GL900282](https://doi.org/10.1029/1998GL900282)
3. V. A. Krasnopolsky, J. P. Maillard, T. C. Owen, Detection of methane in the martian atmosphere: evidence for life? *Icarus* **172**, 537–547 (2004). [doi:10.1016/j.icarus.2004.07.004](https://doi.org/10.1016/j.icarus.2004.07.004)
4. V. Formisano, S. K. Atreya, T. Encrenaz, N. Ignatiev, M. Giuranna, Detection of methane in the atmosphere of Mars. *Science* **306**, 1758–1761 (2004). [doi:10.1126/science.1101732](https://doi.org/10.1126/science.1101732) [Medline](#)
5. S. K. Atreya, P. R. Mahaffy, A. S. Wong, Methane and related trace species on Mars: Origin, loss, implications for life, and habitability. *Planet. Space Sci.* **55**, 358–369 (2007). [doi:10.1016/j.pss.2006.02.005](https://doi.org/10.1016/j.pss.2006.02.005)
6. A. Geminale, V. Formisano, G. Sindoni, Mapping methane in Martian atmosphere with PFS-MEX data. *Planet. Space Sci.* **59**, 137–148 (2011). [doi:10.1016/j.pss.2010.07.011](https://doi.org/10.1016/j.pss.2010.07.011)
7. M. J. Mumma, G. L. Villanueva, R. E. Novak, T. Hewagama, B. P. Bonev, M. A. Disanti, A. M. Mandell, M. D. Smith, Strong release of methane on Mars in northern summer 2003. *Science* **323**, 1041–1045 (2009). [doi:10.1126/science.1165243](https://doi.org/10.1126/science.1165243) [Medline](#)
8. S. Fonti, G. A. Marzo, Mapping the methane on Mars. *Astron. Astrophys.* **512**, A51 (2010). [doi:10.1051/0004-6361/200913178](https://doi.org/10.1051/0004-6361/200913178)
9. V. A. Krasnopolsky, Search for methane and upper limits to ethane and SO₂ on Mars. *Icarus* **217**, 144–152 (2012). [doi:10.1016/j.icarus.2011.10.019](https://doi.org/10.1016/j.icarus.2011.10.019)
10. G. L. Villanueva, M. J. Mumma, R. E. Novak, Y. L. Radeva, H. U. Käufl, A. Smette, A. Tokunaga, A. Khayat, T. Encrenaz, P. Hartogh, A sensitive search for Organics (CH₄, CH₃OH, H₂CO, C₂H₆, C₂H₂, C₂H₄), hydroperoxyl (HO₂), nitrogen Compounds (N₂O, NH₃, HCN) and chlorine species (HCl, CH₃Cl) on Mars using ground-based high-resolution infrared spectroscopy. *Icarus* **223**, 11–27 (2013). [doi:10.1016/j.icarus.2012.11.013](https://doi.org/10.1016/j.icarus.2012.11.013)
11. V. A. Krasnopolsky, A sensitive search for methane and ethane on Mars. *EPSC Abstracts* **6**, 49 (2011).
12. P. R. Mahaffy, C. R. Webster, M. Cabane, P. G. Conrad, P. Coll, S. K. Atreya, R. Arvey, M. Barciniak, M. Benna, L. Bleacher, W. B. Brinckerhoff, J. L. Eigenbrode, D. Carignan, M. Cascia, R. A. Chalmers, J. P. Dworkin, T. Errigo, P. Everson, H. Franz, R. Farley, S. Feng, G. Frazier, C. Freissinet, D. P. Glavin, D. N. Harpold, D. Hawk, V. Holmes, C. S. Johnson, A. Jones, P. Jordan, J. Kellogg, J. Lewis, E. Lyness, C. A. Malespin, D. K. Martin, J. Maurer, A. C. McAdam, D. McLennan, T. J. Nolan, M. Noriega, A. A. Pavlov,

- B. Prats, E. Raaen, O. Sheinman, D. Sheppard, J. Smith, J. C. Stern, F. Tan, M. Trainer, D. W. Ming, R. V. Morris, J. Jones, C. Gundersen, A. Steele, J. Wray, O. Botta, L. A. Leshin, T. Owen, S. Battel, B. M. Jakosky, H. Manning, S. Squyres, R. Navarro-González, C. P. McKay, F. Raulin, R. Sternberg, A. Buch, P. Sorensen, R. Kline-Schoder, D. Coscia, C. Szopa, S. Teinturier, C. Baffes, J. Feldman, G. Flesch, S. Forouhar, R. Garcia, D. Keymeulen, S. Woodward, B. P. Block, K. Arnett, R. Miller, C. Edmonson, S. Gorevan, E. Mumm, The Sample Analysis at Mars Investigation and Instrument Suite. *Space Sci. Rev.* **170**, 401–478 (2012). [doi:10.1007/s11214-012-9879-z](https://doi.org/10.1007/s11214-012-9879-z)
13. C. R. Webster, P. R. Mahaffy, G. J. Flesch, P. B. Nilcs, J. H. Jones, L. A. Leshin, S. K. Atreya, J. C. Stern, L. E. Christensen, T. Owen, H. Franz, R. O. Pepin, A. Steele, C. Achilles, C. Agard, J. A. Alves Verdasca, R. Anderson, R. Anderson, D. Archer, C. Armiens-Aparicio, R. Arvidson, E. Ataskin, A. Aubrey, B. Baker, M. Baker, T. Balic-Zunic, D. Baratoux, J. Baroukh, B. Barraclough, K. Bean, L. Beegle, A. Behar, J. Bell, S. Bender, M. Benna, J. Bentz, G. Berger, J. Berger, D. Berman, D. Bish, D. F. Blake, J. J. Blanco Avalos, D. Blaney, J. Blank, H. Blau, L. Bleacher, E. Boehm, O. Botta, S. Böttcher, T. Boucher, H. Bower, N. Boyd, B. Boynton, E. Breves, J. Bridges, N. Bridges, W. Brinckerhoff, D. Brinza, T. Bristow, C. Brunet, A. Brunner, W. Brunner, A. Buch, M. Bullock, S. Burmeister, M. Cabane, F. Calef, J. Cameron, J. Campbell, B. Cantor, M. Caplinger, J. Caride Rodríguez, M. Carosino, I. Carrasco Blázquez, A. Charpentier, S. Chipera, D. Choi, B. Clark, S. Clegg, T. Cleghorn, E. Cloutis, G. Cody, P. Coll, P. Conrad, D. Coscia, A. Cousin, D. Cremers, J. Crisp, A. Cros, F. Cucinotta, C. d’Uston, S. Davis, M. Day, M. de la Torre Juarez, L. DeFlores, D. DeLapp, J. DeMarines, D. DesMarais, W. Dietrich, R. Dingler, C. Donny, B. Downs, D. Drake, G. Dromart, A. Dupont, B. Duston, J. Dworkin, M. D. Dyar, L. Edgar, K. Edgett, C. Edwards, L. Edwards, B. Ehlmann, B. Ehresmann, J. Eigenbrode, B. Elliott, H. Elliott, R. Ewing, C. Fabre, A. Fairén, K. Farley, J. Farmer, C. Fassett, L. Favot, D. Fay, F. Fedosov, J. Feldman, S. Feldman, M. Fisk, M. Fitzgibbon, M. Floyd, L. Flückiger, O. Forni, A. Fraeman, R. Francis, P. François, C. Freissinet, K. L. French, J. Frydenvang, A. Gaboriaud, M. Gailhanou, J. Garvin, O. Gasnault, C. Geffroy, R. Gellert, M. Genzer, D. Glavin, A. Godber, F. Goesmann, W. Goetz, D. Golovin, F. Gómez Gómez, J. Gómez-Elvira, B. Gondet, S. Gordon, S. Gorevan, J. Grant, J. Griffes, D. Grinspoon, J. Grotzinger, P. Guillemot, J. Guo, S. Gupta, S. Guzewich, R. Haberle, D. Halleaux, B. Hallet, V. Hamilton, C. Hardgrove, D. Harker, D. Harpold, A. M. Harri, K. Harshman, D. Hassler, H. Haukka, A. Hayes, K. Herkenhoff, P. Herrera, S. Hettrich, E. Heydari, V. Hipkin, T. Hoehler, J. Hollingsworth, J. Hudgins, W. Huntress, J. Hurowitz, S. Hviid, K. Iagnemma, S. Indyk, G. Israël, R. Jackson, S. Jacob, B. Jakosky, E. Jensen, J. K. Jensen, J. Johnson, M. Johnson, S. Johnstone, A. Jones, J. Joseph, I. Jun, L. Kah, H. Kahanpää, M. Kahre, N. Karpushkina, W. Kasprzak, J. Kauhanen, L. Keely, O. Kempainen, D. Keymeulen, M. H. Kim, K. Kinch, P. King, L. Kirkland, G. Kocurek, A. Koefoed, J. Köhler, O. Kortmann, A. Kozyrev, J. Krezoski, D. Krysak, R. Kuzmin, J. L. Lacour, V. Lafaille, Y. Langevin, N. Lanza, J. Lasue, S. Le Mouélic, E. M. Lee, Q. M. Lee, D. Lees, M. Lefavor, M. Lemmon, A. Lepinette Malvitte, R. Léveillé, É. Lewin-Carpintier, K. Lewis, S. Li, L. Lipkaman, C. Little, M. Litvak, E. Lorigny, G. Lugmair, A. Lundberg, E. Lyness, M. Madsen, J. Maki, A. Malakhov, C. Malespin, M. Malin, N. Mangold, G. Manhes, H. Manning, G. Marchand, M. Marín Jiménez, C. Martín García, D. Martin, M. Martin, J. Martínez-Frías, J. Martín-Soler, F. J. Martín-Torres, P. Mauchien, S. Maurice,

A. McAdam, E. McCartney, T. McConnochie, E. McCullough, I. McEwan, C. McKay, S. McLennan, S. McNair, N. Melikechi, P. Y. Meslin, M. Meyer, A. Mezzacappa, H. Miller, K. Miller, R. Milliken, D. Ming, M. Minitti, M. Mischna, I. Mitrofanov, J. Moersch, M. Mokrousov, A. Molina Jurado, J. Moores, L. Mora-Sotomayor, J. M. Morookian, R. Morris, S. Morrison, R. Mueller-Mellin, J. P. Muller, G. Muñoz Caro, M. Nachon, S. Navarro López, R. Navarro-González, K. Nealson, A. Nefian, T. Nelson, M. Newcombe, C. Newman, H. Newsom, S. Nikiforov, B. Nixon, E. Noe Dobrea, T. Nolan, D. Oehler, A. Ollila, T. Olson, M. Á. de Pablo Hernández, A. Paillet, E. Pallier, M. Palucis, T. Parker, Y. Parot, K. Patel, M. Paton, G. Paulsen, A. Pavlov, B. Pavri, V. Peinado-González, L. Peret, R. Perez, G. Perrett, J. Peterson, C. Pilorget, P. Pinet, J. Pla-García, I. Plante, F. Poitrasson, J. Polkko, R. Popa, L. Posiolova, A. Posner, I. Pradler, B. Prats, V. Prokhorov, S. W. Purdy, E. Raaen, L. Radziemski, S. Rafkin, M. Ramos, E. Rampe, F. Raulin, M. Ravine, G. Reitz, N. Rennó, M. Rice, M. Richardson, F. Robert, K. Robertson, J. A. Rodriguez Manfredi, J. J. Romeral-Planelló, S. Rowland, D. Rubin, M. Saccoccio, A. Salamon, J. Sandoval, A. Sanin, S. A. Sans Fuentes, L. Saper, P. Sarrazin, V. Sautter, H. Savijärvi, J. Schieber, M. Schmidt, W. Schmidt, D. Scholes, M. Schoppers, S. Schröder, S. Schwenzer, E. Sebastian Martinez, A. Sengstacken, R. Shterts, K. Siebach, T. Siili, J. Simmonds, J. B. Sirven, S. Slavney, R. Sletten, M. Smith, P. Sobrón Sánchez, N. Spanovich, J. Spray, S. Squyres, K. Stack, F. Stalport, T. Stein, N. Stewart, S. L. Stipp, K. Stoiber, E. Stolper, B. Sucharski, R. Sullivan, R. Summons, D. Sumner, V. Sun, K. Supulver, B. Sutter, C. Szopa, F. Tan, C. Tate, S. Teinturier, I. ten Kate, P. Thomas, L. Thompson, R. Tokar, M. Toplis, J. Torres Redondo, M. Trainer, A. Treiman, V. Tretyakov, R. Urqui-O'Callaghan, J. Van Beek, T. Van Beek, S. VanBommel, D. Vaniman, A. Varenikov, A. Vasavada, P. Vasconcelos, E. Vicenzi, A. Vostrukhin, M. Voytek, M. Wadhwa, J. Ward, E. Weigle, D. Wellington, F. Westall, R. C. Wiens, M. B. Wilhelm, A. Williams, J. Williams, R. Williams, R. B. Williams, M. Wilson, R. Wimmer-Schweingruber, M. Wolff, M. Wong, J. Wray, M. Wu, C. Yana, A. Yen, A. Yingst, C. Zeitlin, R. Zimdar, M. P. Zorzano Mier; MSL Science Team, Isotope ratios of H, C, and O in CO₂ and H₂O of the martian atmosphere. *Science* **341**, 260–263 (2013). [doi:10.1126/science.1237961](https://doi.org/10.1126/science.1237961) [Medline](#)

14. Materials and methods are available as supplementary materials on *Science* Online.

15. F. Lefèvre, F. Forget, Observed variations of methane on Mars unexplained by known atmospheric chemistry and physics. *Nature* **460**, 720–723 (2009). [doi:10.1038/nature08228](https://doi.org/10.1038/nature08228) [Medline](#)

16. A. S. Wong, S. K. Atreya, T. Encrenaz, Chemical markers of possible hot spots on Mars. *J. Geophys. Res.* **108**, (E4), 5026 (2003). [doi:10.1029/2002JE002003](https://doi.org/10.1029/2002JE002003)

17. K. J. Zahnle, R. S. Freedman, D. C. Catling, Is there methane on Mars? *Icarus* **212**, 493–503 (2011). [doi:10.1016/j.icarus.2010.11.027](https://doi.org/10.1016/j.icarus.2010.11.027)

18. R. A. Kerr, Planetary science. Question of martian methane is still up in the air. *Science* **338**, 733 (2012). [doi:10.1126/science.338.6108.733](https://doi.org/10.1126/science.338.6108.733) [Medline](#)

19. V. A. Krasnopolsky, Some problems related to the origin of methane on Mars. *Icarus* **180**, 359–367 (2006). [doi:10.1016/j.icarus.2005.10.015](https://doi.org/10.1016/j.icarus.2005.10.015)

20. P. R. Christensen, Mars as seen from the 2001 Mars Odyssey Thermal Emission Imaging System experiment. *EOS Trans. AGU Fall Meet. Suppl.* **84** (46), Abstract P21A-02, 2003.
21. T. Encrenaz, T. K. Greathouse, M. J. Richter, J. H. Lacy, T. Fouchet, B. Bézard, F. Lefèvre, F. Forget, S. K. Atreya, A stringent upper limit to SO₂ in the Martian atmosphere. *Astron. Astrophys.* **530**, 1–5 (2011). [doi:10.1051/0004-6361/201116820](https://doi.org/10.1051/0004-6361/201116820)
22. S. K. Atreya, O. Witasse, V. F. Chevrier, F. Forget, P. R. Mahaffy, P. Buford Price, C. R. Webster, R. W. Zurek, Methane on Mars: Current observations, interpretation, and future plans. *Planet. Space Sci.* **59**, 133–136 (2011). [doi:10.1016/j.pss.2010.10.008](https://doi.org/10.1016/j.pss.2010.10.008)
23. S. K. Atreya, A. S. Wong, N. O. Renno, W. M. Farrell, G. T. Delory, D. D. Sentman, S. A. Cummer, J. R. Marshall, S. C. Rafkin, D. C. Catling, Oxidant enhancement in martian dust devils and storms: implications for life and habitability. *Astrobiology* **6**, 439–450 (2006). [doi:10.1089/ast.2006.6.439](https://doi.org/10.1089/ast.2006.6.439) [Medline](#)
24. G. T. Delory, W. M. Farrell, S. K. Atreya, N. O. Renno, A. S. Wong, S. A. Cummer, D. D. Sentman, J. R. Marshall, S. C. Rafkin, D. C. Catling, Oxidant enhancement in martian dust devils and storms: storm electric fields and electron dissociative attachment. *Astrobiology* **6**, 451–462 (2006). [doi:10.1089/ast.2006.6.451](https://doi.org/10.1089/ast.2006.6.451) [Medline](#)
25. W. M. Farrell, G. T. Delory, S. K. Atreya, Martian Dust Storms as a Possible Sink of Atmospheric Methane. *J. Geophys. Res.* **33**, (2006). [10.1029/2006GL027210](https://doi.org/10.1029/2006GL027210)
26. L. S. Rothman, I. E. Gordon, A. Barbe, D. C. Benner, P. F. Bernath, M. Birk, V. Boudon, L. R. Brown, A. Campargue, J.-P. Champion, K. Chance, L. H. Coudert, V. Dana, V. M. Devi, S. Fally, J.-M. Flaud, R. R. Gamache, A. Goldman, D. Jacquemart, I. Kleiner, N. Lacome, W. J. Lafferty, J.-Y. Mandin, S. T. Massie, S. N. Mikhailenko, C. E. Miller, N. Moazzen-Ahmadi, O. V. Naumenko, A. V. Nikitin, J. Orphal, V. I. Perevalov, A. Perrin, A. Predoi-Cross, C. P. Rinsland, M. Rotger, M. Šimečková, M. A. H. Smith, K. Sung, S. A. Tashkun, J. Tennyson, R. A. Toth, A. C. Vandaele, J. Vander Auwera, The HITRAN 2008 Molecular Spectroscopic Database. *J. Quant. Spectrosc. Radiat. Transf.* **110**, 533–572 (2009). [doi:10.1016/j.jqsrt.2009.02.013](https://doi.org/10.1016/j.jqsrt.2009.02.013)
27. C. R. Webster, R. T. Menzies, E. D. Hinkley, “Infrared laser absorption: theory and applications,” *Laser Remote Chemical Analysis*, R.M. Measures, ed., Wiley, New York, Chap. 3, (1988).